

Ferroelectricity in nonstoichiometric SrTiO₃ films studied by ultraviolet Raman spectroscopy

D. A. Tenne, A. K. Farrar, C. M. Brooks, T. Heeg, J. Schubert, H. W. Jang, C. W. Bark, C. M. Folkman, C. B. Eom, and D. G. Schlom

Citation: [Appl. Phys. Lett.](#) **97**, 142901 (2010); doi: 10.1063/1.3499273

View online: <https://doi.org/10.1063/1.3499273>

View Table of Contents: <http://aip.scitation.org/toc/apl/97/14>

Published by the [American Institute of Physics](#)

Articles you may be interested in

[Growth of homoepitaxial SrTiO₃ thin films by molecular-beam epitaxy](#)

Applied Physics Letters **94**, 162905 (2009); 10.1063/1.3117365

[Tuning thermal conductivity in homoepitaxial SrTiO₃ films via defects](#)

Applied Physics Letters **107**, 051902 (2015); 10.1063/1.4927200

[Bulk electronic structure of SrTiO₃: Experiment and theory](#)

Journal of Applied Physics **90**, 6156 (2001); 10.1063/1.1415766

[Raman Spectrum of Strontium Titanate](#)

The Journal of Chemical Physics **48**, 2240 (1968); 10.1063/1.1669418

[Observation of room-temperature ferroelectricity in tetragonal strontium titanate thin films on SrTiO₃ \(001\) substrates](#)

Applied Physics Letters **91**, 042908 (2007); 10.1063/1.2764437

[Growth of high-quality SrTiO₃ films using a hybrid molecular beam epitaxy approach](#)

Journal of Vacuum Science & Technology A: Vacuum, Surfaces, and Films **27**, 461 (2009); 10.1116/1.3106610



Instruments for Advanced Science

Contact Hiden Analytical for further details:

W www.HidenAnalytical.com

E info@hiden.co.uk

CLICK TO VIEW our product catalogue



Gas Analysis

- dynamic measurement of reaction gas streams
- catalysis and thermal analysis
- molecular beam studies
- dissolved species probes
- fermentation, environmental and ecological studies



Surface Science

- UHV TPD
- SIMS
- end point detection in ion beam etch
- elemental imaging - surface mapping



Plasma Diagnostics

- plasma source characterization
- etch and deposition process reaction
- kinetic studies
- analysis of neutral and radical species



Vacuum Analysis

- partial pressure measurement and control of process gases
- reactive sputter process control
- vacuum diagnostics
- vacuum coating process monitoring

Ferroelectricity in nonstoichiometric SrTiO_3 films studied by ultraviolet Raman spectroscopy

D. A. Tenne,^{1,a)} A. K. Farrar,¹ C. M. Brooks,^{2,3} T. Heeg,³ J. Schubert,⁴ H. W. Jang,⁵
C. W. Bark,⁵ C. M. Folkman,⁵ C. B. Eom,⁵ and D. G. Schlom³

¹Department of Physics, Boise State University, 1910 University Drive, Boise, Idaho 83725-1570, USA

²Department of Materials Science and Engineering, The Pennsylvania State University, University Park, Pennsylvania 16802-5005, USA

³Department of Materials Science and Engineering, Cornell University, Ithaca, New York 14853-1501, USA

⁴Institute of Bio and Nanosystems, JARA-Fundamentals of Future Information Technologies, Research Centre Jülich, D-52425 Jülich, Germany

⁵Department of Materials Science and Engineering, University of Wisconsin, Madison, Wisconsin 53706, USA

(Received 9 August 2010; accepted 18 September 2010; published online 5 October 2010)

Homoepitaxial $\text{Sr}_{1+x}\text{TiO}_{3+\delta}$ films with $-0.2 \leq x \leq 0.25$ grown by reactive molecular-beam epitaxy on SrTiO_3 (001) substrates have been studied by ultraviolet Raman spectroscopy. Nonstoichiometry for strontium-deficient compositions leads to the appearance of strong first-order Raman scattering at low temperatures, which decreases with increasing temperature and disappears at about 350 K. This indicates the appearance of a spontaneous polarization with a paraelectric-to-ferroelectric transition temperature above room temperature. Strontium-rich samples also show a strong first-order Raman signal, but the peaks are significantly broader and exhibit a less pronounced temperature dependence, indicating a stronger contribution of the disorder-activated mechanism in Raman scattering. © 2010 American Institute of Physics. [doi:10.1063/1.3499273]

SrTiO_3 is a well known incipient ferroelectric, and in bulk remains paraelectric down to 0.3 K.¹ Slight perturbations in the lattice structure can, however, break the delicate balance of forces and lead to the appearance of ferroelectric polarization. This perturbation can come from various sources such as strain,^{2–5} doping,^{6–8} or even oxygen isotope substitution.⁹ Here we focus on the effect of Sr/Ti nonstoichiometry in homoepitaxial SrTiO_3 thin films. Specifically of interest is how variation in stoichiometry affects the phonons and their activity in Raman spectra resulting from the ferroelectric phase transitions. Raman spectroscopy is a powerful tool for probing lattice vibrations. For thin films of wide band gap materials such as SrTiO_3 , excitation using ultraviolet (UV) light is preferable, since UV light with energy above the band gap (3.2 eV for SrTiO_3 at 300 K) is absorbed, and therefore the substrate signal is strongly suppressed allowing measurement of spectra from ferroelectric films as thin as a few nanometers.^{10,11} In this paper, we apply UV Raman spectroscopy to study ferroelectricity in nonstoichiometric (both strontium-rich and strontium-deficient) homoepitaxial SrTiO_3 films.

The 100-nm-thick films were grown by molecular-beam epitaxy (MBE) on stoichiometric, TiO_2 -terminated (001) SrTiO_3 substrates at 650 °C in a background pressure of 5.0×10^{-7} Torr of ultrahigh purity molecular oxygen. Growth was monitored by reflection high-energy electron diffraction. Six $\text{Sr}_{1+x}\text{TiO}_{3+\delta}$ films were studied; nominal compositions x varied from -0.2 to 0.3 , including a stoichiometric film, $x=0$. The Sr/Ti concentration ratios ($1+x$) were determined by Rutherford backscattering spectrometry (RBS) to be 0.786, 0.905, 0.97, 1.02, 1.19, and 1.24, resulting in x values -0.214 , -0.095 , -0.03 , 0.02 , 0.19 , and 0.24 (± 0.04), close to the nominal ones. There may be a certain

amount of oxygen nonstoichiometry δ but the oxygen concentration in the films is difficult to determine by RBS due to the low atomic mass of oxygen. The details of growth and structural characterization by x-ray diffraction (XRD) and scanning transmission electron microscopy (STEM) have been reported elsewhere.¹² According to STEM images, the strontium deficient films appear to have a disordered structure (randomly distributed defects); no secondary phases like TiO_2 were detected. In the strontium excess films, the Ruddlesden–Popper planar faults appear.¹² Both Sr-deficient and Sr-rich films have shown an expansion along the c axis; the c lattice parameters determined by XRD were 3.94 Å, 3.915 Å, 3.905 Å, 3.92 Å, 3.96 Å, and 4.02 Å, respectively, for the compositions listed above.¹² Since the films were homoepitaxial, any effect of substrate-induced strain should be negligible. Also, spectra of nominally stoichiometric SrTiO_3 films grown by pulsed-laser deposition (PLD) on SrTiO_3 substrates with and without SrRuO_3 buffer layers were measured. The PLD growth details were reported elsewhere.¹³

Raman spectra were recorded using a Horiba Jobin Yvon T64000 triple spectrometer equipped with a liquid-nitrogen-cooled multichannel charge-coupled device detector. Spectra were recorded in backscattering geometry in the temperature range 10–450 K using a variable temperature closed cycle He cryostat. For excitation, the 325 nm He–Cd laser line was used with a power density of 0.5 W/mm² at the sample surface, low enough to avoid any noticeable local heating.¹⁴

SrTiO_3 is a cubic perovskite-type crystal having 12 optical phonon modes. All phonons are of an odd symmetry with respect to the inversion, hence inactive in the first-order Raman scattering. Raman spectrum of bulk SrTiO_3 contains only the second order (two-phonon) features.¹⁵ A breakdown in the inversion symmetry of the crystal (e.g., due to a ferroelectric distortion) leads to the appearance of the first-order peaks Raman spectra.

^{a)}Electronic mail: dmitritenne@boisestate.edu.

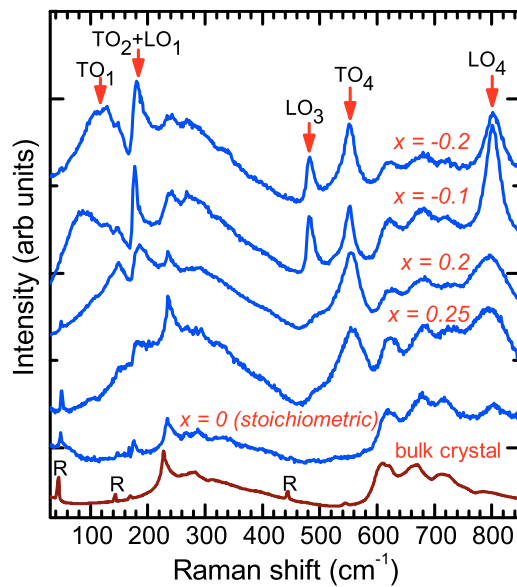


FIG. 1. (Color online) Raman spectra of $\text{Sr}_{1+x}\text{TiO}_{3+\delta}$ films and a bulk SrTiO_3 crystal at 10 K. Arrows mark the first-order SrTiO_3 phonon peaks. Symbols "R" label the structural modes due to the rotation of the Ti-O octahedra.

Figure 1 shows Raman spectra of a bulk SrTiO_3 crystal, the MBE-grown stoichiometric film, and nonstoichiometric films at 10 K. The stoichiometric film's spectrum is similar to bulk SrTiO_3 with broad second order peaks. The structural modes at 44, 144, and 445 cm^{-1} (labeled R in Fig. 1) present in the low-temperature spectra are due to the antiferrodistortive cubic-tetragonal phase transition, which occurs at 105 K and involves the rotation of the Ti-O octahedra.¹⁶ The resulting tetragonal structure $4/mmm$ is still centrosymmetric and the fundamental SrTiO_3 phonons remain Raman inactive. In contrast, the nonstoichiometric films exhibit intensive first-order peaks of the fundamental SrTiO_3 phonons, indicative of a breakdown in inversion symmetry. The spectral features that we focus on are TO_1 (the soft mode) at 85–120 cm^{-1} , and the hard modes TO_2+LO_1 (these two modes have very close frequencies), LO_3 , TO_4 , and LO_4 at 180 cm^{-1} , 480 cm^{-1} , 550 cm^{-1} , and 800 cm^{-1} , respectively.

Variable temperature spectra of strontium-deficient films [Fig. 2(a)] showed these peaks decreasing and disappearing at ~ 350 K. The complete disappearance of the first-order Raman peaks at higher temperatures indicates that the breakdown of the inversion symmetry selection rules cannot be attributed to lattice defects alone. If the first-order Raman scattering is defect-induced, it should be observed at higher temperatures as well. At higher temperatures (above 350 K), however, the spectra of strontium-deficient films are the same as stoichiometric SrTiO_3 . The observed behavior indicates the appearance of spontaneous polarization in the strontium-deficient films. Considering the temperature evolution of the spectra of strontium-rich films [Fig. 2(b)], one can notice a different behavior as follows: even at low temperatures the phonon peaks are broad (about twice as broad compared to the strontium-deficient films), and they do not disappear even at high temperatures. This indicates a stronger contribution of the defect-induced mechanism in Raman scattering in the strontium-rich films.

The breakdown of the symmetry selection rules has been previously observed in Raman scattering from SrTiO_3 films

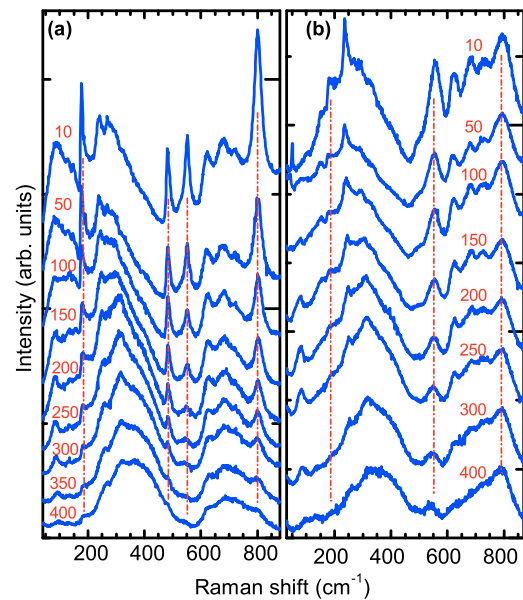


FIG. 2. (Color online) Variable-temperature Raman spectra of a Sr-deficient $\text{Sr}_{0.9}\text{TiO}_{3+\delta}$ film (a) and a Sr-rich $\text{Sr}_{1.25}\text{TiO}_{3+\delta}$ film (b). Numbers above the spectra indicate temperatures in K. The vertical dashed-dotted lines are guides for the eye showing the first-order SrTiO_3 phonon peaks.

grown by PLD,¹⁷ and attributed to polar nanoregions associated with oxygen vacancies¹⁷ or dipole moments associated with polar grain boundaries in polycrystalline or textured samples.¹⁸ The samples studied here are single-crystalline films having no grain boundaries, so this effect is not present. Later studies of intentionally oxygen-reduced bulk SrTiO_3 showed that oxygen vacancies alone are unlikely to cause the observed effect, and should also lead to the appearance of additional peaks, that are not present in the thin film spectra.¹⁹ Even if oxygen vacancies play a role, it must be in combination with other nonstoichiometry or defects.

Figure 3 shows Raman spectra of strontium-deficient film and two nominally stoichiometric PLD-grown SrTiO_3

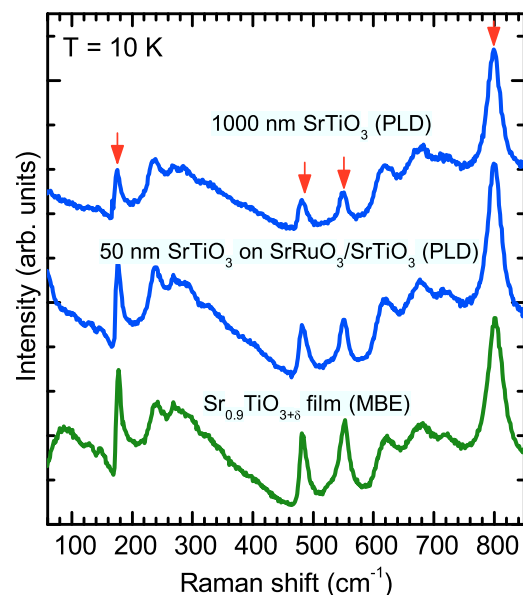


FIG. 3. (Color online) Raman spectra of the strontium-deficient MBE-grown film ($\text{Sr}_{0.9}\text{TiO}_{3+\delta}$) and two nominally stoichiometric SrTiO_3 films grown by PLD on SrTiO_3 substrates with and without SrRuO_3 buffer layers. Arrows indicate the first-order peaks of the SrTiO_3 optical phonons.

films on SrTiO₃ substrates without and with SrRuO₃ buffer layers. The latter films (with SrRuO₃ bottom electrodes) were proved to be ferroelectric by a combination of techniques including the polarization hysteresis loops measured by piezoresponse force microscopy.¹³ The shape and temperature evolution of Raman spectra from SrTiO₃ films with and without SrRuO₃ contact layers are essentially the same. This indicates that thin coherently strained SrRuO₃ layers following the lattice parameter of the SrTiO₃ substrate have no noticeable effect on the properties of SrTiO₃ films. The spectra of the strontium-deficient films studied here are remarkably similar to the spectra of the PLD-grown ferroelectric SrTiO₃ in terms of both the first-order Raman peaks (which are slightly stronger in the strontium-deficient films) and their temperature evolution (Fig. 3). This result supports the suggestion that relatively small amounts of cation nonstoichiometry, which were demonstrated to occur even in nominally stoichiometric PLD-grown samples,^{20,21} can lead to the appearance of polar nanoregions and relaxorlike ferroelectricity, as reported by Jang *et al.*¹³

In summary, Sr/Ti nonstoichiometry in homoepitaxial SrTiO₃ films leads to the appearance of first-order peaks in Raman spectra, which are symmetry-forbidden in paraelectric SrTiO₃. Strontium-deficient samples, in particular, exhibit a temperature evolution of Raman spectra consistent with a ferroelectric phase transition with the transition temperature ~ 350 K. Similar spectra have been recorded from nominally stoichiometric PLD samples proven to be ferroelectric. Our results highlight the sensitive nature of the ferroelectric properties of SrTiO₃ to stoichiometry and imply that strontium deficiency (probably existing in small amounts even in nominally stoichiometric SrTiO₃ films and single crystals) can offer an explanation for the origin of polar nanoregions.

This work was supported in part by the NSF through Grant Nos. DMR-0705127 (D.A.T.), DMR-0507146 (D.G.S.), ECCS-0708759 (C.B.E.), and DMR-0906443 (C.B.E.) and through the MRSEC program by Grant No. DMR-0820404 (C.M.B), DOE EPSCoR Grant No. DE-FG02-04ER46142 (D.A.T.), and Research Corporation for Science Advancement Grant No. 7134 (D.A.T.).

- ¹K. A. Müller and H. Burkard, *Phys. Rev. B* **19**, 3593 (1979).
- ²W. J. Burke and R. J. Pressley, *Solid State Commun.* **9**, 191 (1971).
- ³H. Uwe and T. Sakudo, *Phys. Rev. B* **13**, 271 (1976).
- ⁴N. A. Pertsev, A. K. Tagantsev, and N. Setter, *Phys. Rev. B* **61**, R825 (2000).
- ⁵J. H. Haeni, P. Irvin, W. Chang, R. Uecker, P. Reiche, Y. L. Li, S. Choudhury, W. Tian, M. E. Hawley, B. Craigo, A. K. Tagantsev, X. Q. Pan, S. K. Streiffer, L. Q. Chen, S. W. Kirchoefer, J. Levy, and D. G. Schlom, *Nature (London)* **430**, 758 (2004).
- ⁶T. Mitsui and W. B. Westphal, *Phys. Rev.* **124**, 1354 (1961).
- ⁷J. G. Bednorz and K. A. Müller, *Phys. Rev. Lett.* **52**, 2289 (1984).
- ⁸U. Bianchi, W. Kleemann, and J. C. Bednorz, *J. Phys.: Condens. Matter* **6**, 1229 (1994).
- ⁹M. Itoh, R. Wang, Y. Inaguma, T. Yamaguchi, Y. J. Shan, and T. Nakamura, *Phys. Rev. Lett.* **82**, 3540 (1999).
- ¹⁰D. A. Tenne, A. Bruchhausen, N. D. Lanzillotti-Kimura, A. Fainstein, R. S. Katiyar, A. Cantarero, A. Soukiassian, V. Vaithyanathan, J. H. Haeni, W. Tian, D. G. Schlom, K. J. Choi, D. M. Kim, C. B. Eom, H. P. Sun, X. Q. Pan, Y. L. Li, L. Q. Chen, Q. X. Jia, S. M. Nakhmanson, K. M. Rabe, and X. X. Xi, *Science* **313**, 1614 (2006).
- ¹¹D. A. Tenne, P. Turner, J. D. Schmidt, M. Biegalski, Y. L. Li, L. Q. Chen, A. Soukiassian, S. Troler-McKinstry, D. G. Schlom, X. X. Xi, D. D. Fong, P. H. Fuoss, J. A. Eastman, G. B. Stephenson, C. Thompson, and S. K. Streiffer, *Phys. Rev. Lett.* **103**, 177601 (2009).
- ¹²C. M. Brooks, L. Fitting Kourkoutis, T. Heeg, J. Schubert, D. A. Muller, and D. G. Schlom, *Appl. Phys. Lett.* **94**, 162905 (2009).
- ¹³H. W. Jang, A. Kumar, S. Denev, M. D. Biegalski, P. Maksymovych, C. W. Bark, C. T. Nelson, C. M. Folkman, S. H. Baek, N. Balke, C. M. Brooks, D. A. Tenne, D. G. Schlom, L. Q. Chen, X. Q. Pan, S. V. Kalinin, V. Gopalan, and C. B. Eom, *Phys. Rev. Lett.* **104**, 197601 (2010).
- ¹⁴See supporting online material for Tenne *et al.* (Ref. 10).
- ¹⁵W. G. Nilsen and J. G. Skinner, *J. Chem. Phys.* **48**, 2240 (1968).
- ¹⁶P. A. Fleury, J. F. Scott, and J. M. Worlock, *Phys. Rev. Lett.* **21**, 16 (1968).
- ¹⁷A. A. Sirenko, I. A. Akimov, J. R. Fox, A. M. Clark H.-C. Li, W. Si, and X. X. Xi, *Phys. Rev. Lett.* **82**, 4500 (1999).
- ¹⁸J. Petzelt, T. Ostapchuk, I. Gregora, I. Rychetský, S. Hoffmann-Eifert, A. V. Pronin, Y. Yuzyuk, B. P. Gorshunov, S. Kamba, V. Bovtun, J. Pokorný, M. Savinov, V. Porokhonsky, D. Rafaja, P. Vaněk, A. Almeida, M. R. Chaves, A. A. Volkov, M. Dressel, and R. Waser, *Phys. Rev. B* **64**, 184111 (2001).
- ¹⁹D. A. Tenne, I. E. Gonenli, A. Soukiassian, D. G. Schlom, S. M. Nakhmanson, K. M. Rabe, and X. X. Xi, *Phys. Rev. B* **76**, 024303 (2007).
- ²⁰T. Ohnishi, K. Shibuya, T. Yamamoto, and M. Lippmaa, *J. Appl. Phys.* **103**, 103703 (2008).
- ²¹D. J. Keeble, R. A. Mackie, W. Egger, B. Löwe, P. Pikart, C. Hugenschmidt, and T. J. Jackson, *Phys. Rev. B* **81**, 064102 (2010).